湖南大学学报（自然科学版）
Journal of Hunan University (Natural Sciences)

第 50 卷 第 6 期
2023 年 6 月

Available online at http://jonuns.com/index.php/journal/index

Vol. 50 No. 6
June 2023

Open Access Article https://doi.org/10.55463/issn.1674-2974.50.6.2

Optical Properties of Chalcogenide Thin Films for Solar Cells

Yordanka Trifonova[1]*, Vanya Lilova[1], Vladislava Ivanova[1], Teodora Stoyanova Lyubenova[2], Plamen Petkov[1]

[1] Department of Physics, University of Chemical Technology and Metallurgy, 8 Kliment Ohridski Blvd., Sofia, 1756, Bulgaria

[2] Department of Inorganic and Organic Chemistry, University Jaume I, Av. Sos Baynat, Castellón de la Plana, 12071, Spain

* Corresponding author: danche@uctm.edu

Received: March 4, 2023 / Revised: April 1, 2023 / Accepted: May 5, 2023 / Published: June 30, 2023

Abstract: The aim of this paper is to study the optical properties of thin films with composition $Cu_{0.9}(In_{0.7}Ga_{0.3})Se_2$ (CIGS) for a photovoltaic solar cell absorber. Samples with different film thicknesses were prepared using the doctor blade technique of previously co-precipitated aqueous precursors. The materials were characterized by X-ray diffraction (XRD) and scanning electron microscopy (SEM). For the first time, the optical properties of the thin layers with this composition, obtained using the doctor blade technique, were investigated. The optical properties were studied by transmittance and reflectance measurements in the infrared region and are correlated with film thickness. The dependence of the absorption coefficient on wavelength and the energy gap was found to be affected by the layer depth. The greater absorption coefficient is related to thinner CIGS layer. The refractive index results in an abnormal dispersion. The optical band gap was also determined in accordance with the sample chemical composition.

Keywords: chalcogenide films, optical properties, optical band gap, refractive index, absorption coefficient.

太阳能电池用硫族化物薄膜的光学特性

摘要：本文的目的是研究用于光伏太阳能电池吸收器的 Cu0.9(In0.7Ga0.3)Se2 (CIGS) 薄膜的光学特性。使用预先共沉淀的水性前体的刮刀技术制备具有不同膜厚度的样品。通过 X 射线衍射(X 射线衍射)和扫描电子显微镜(扫描电镜)对材料进行了表征。首次研究了使用刮刀技术获得的具有该组合物的薄层的光学性质。通过红外区域的透射率和反射率测量来研究光学特性，并与薄膜厚度相关。发现吸收系数对波长和能隙的依赖性受到层深度的影响。较大的吸收系数与较薄的 CIGS 层有关。折射率导致异常色散。光学带隙也根据样品的化学成分确定。

关键词：硫族化物薄膜，光学性能，光学带隙，折射率，吸收系数。

Introduction

Solar cells based on chalcogenide materials are widely considered one of the most promising technologies because of their long-term stability [1]

and high values of efficient conversion of solar energy. CIGS based thin films are considered as the most promising material because of their high stability against photo degradation [2], high efficiency and optical absorption in the visible spectrum. The best solar cells based on Cu(In, Ga)(Se, S)$_2$ materials (non-tandem device) have been recently reported with 22.9% conversion efficiency [3-7]. The energy efficiency of the layers studied is 7.2% [8]. Therefore, we investigated their optical properties to determine the possibility of increasing energy efficiency and the areas of application.

High vacuum-based processes like co-evaporation or magnetic sputtering usually deposit CIGS high-efficiency devices [9-13]. Many attempts have been made to fabricate CIGS films by non-vacuum methods such as chemical spray deposition [14], spray pyrolysis [15], ink print techniques [16-18], electrodeposition [19-22], pulsed laser deposition [23], chemical bath deposition [24], and soft-chemistry synthesis routes [8, 25]. The non-vacuum techniques do not reach the same high efficiencies as the vacuum processes, but they provide lower costs, better large area homogeneity and this would make them highly competitive for future applications at industrial scale.

Therefore, it is important to find a suitable film deposition method because all vacuum deposition techniques are heavy and expensive. Non-vacuum techniques such as electrodeposition do not reach the same high efficiencies as the vacuum processes, but they provide lower costs, better large area homogeneity [26].

The present work contributes to the field of the optical properties of CIGS thin films deposed by one of the widely used techniques for producing thin films on large area surfaces, the so-called doctor blade or tape casting technique [27]. This deposition was chosen as a low-cost, re-scalable on future large industrial scale, and simple way of layer preparation as no specific equipment was required. It consisted of knife spreading of slurry onto casting surface. In this study, the surface was stationary, and the blade was mobile. The thickness of the layers is determined by adjusting the gap between the blade and the substrate by modifying the rheological properties of the slurry. Thin film deposition and precursor synthesis are essential steps for tailoring optical and electrical properties of photovoltaic (PV) absorbers. The influence of chemical composition, film thickness, and layer morphology is evaluated in terms of layer optical response.

1. Experiment

1.1. Sample Preparation

In the present work, the CIGS compound was planned as a solid solution $Cu_{0.9}In_{0.7}Ga_{0.3}Se_2$ with a metal ratio of [Cu]/([In] + [Ga]) = 0.9 and [Ga]/([In] + [Ga]) = 0.3 [28].

The chemicals applied to the preparation of the CIGS absorber were $Cu(NO_3)_{2.3}H_2O$ (99%, Sigma Aldrich), $In(NO_3)_3$ (98%, Aldrich), $Ga(NO_3)3$ (99.9%, Aldrich), SeO_2 (99.8%, Acros), NH_4OH (25%, Panreac). They were used as received without further purification. Precursor solution was obtained by dissolving copper ($2.52x10^{-3}$ mol), indium ($1.96x10^{-3}$ mol) and gallium ($0.84x10^{-3}$ mol) nitrates in 125 cm^3 of distilled water with a final metal ratio of [Cu]/([In]+[Ga]) = 0.9 and [Ga]/([In]+[Ga]) = 0.3 [8].

Separately, $10x10^{-3}$ mol SeO_2 was dissolved in distilled water, resulting in colorless transparent solution. The two solutions obtained were mixed at stirring. The pH of the mixed solution was determined to be pH = 6 (neutral solution). Ammonia was added in a single batch to obtain the desired metal selenium precipitate. The resulting powder was washed with water and ethanol, filtered and dried.

1.2. Thin Film Preparation

To make the ink, triethanolamine as surfactant and reducer ($C_6H_{15}NO_3$) and ethanol (C_2H_5OH) were used. The obtained paste was deposited by a simplified doctor blade method (knife coating) on soda-lime glass substrates. Two samples were prepared: sample V1 with two layers and sample V2 with tree layers. The obtained layers were pre-heated on a hot plate at 400°C for 2 min to partially remove the solvent, for further precursor decomposition, and selenite reduction [8]. Finally, the CIGS films were selenized using elemental Se under Ar atmosphere in a tubular furnace. The applied thermal cycle corresponds to a heating velocity rate of 20ºC/min up to a maximum temperature of 525ºC. Elemental selenium powder (Se, 99.5%, Merck) was introduced separately into the furnace as a selenium source to prevent Se volatilization during the treatment.

1.3. Thin Film Characterization

1.3.1. X-Ray Diffraction

The crystal structure of the materials was analyzed by X-ray powder diffraction (XRD) with a Siemens D5000D diffractometer. The data were collected by step-scanning from 10 to 80º 2θ with a step size of 0.05º 2θ and 1s counting time per step. The particle size was calculated using the Scherer formula:

$$D_p = \frac{0.94 \times \lambda}{\beta \times \cos\theta} \quad (1)$$

where D_p is the average crystallite size, β - line broadening in radians, θ – the Bragg angle, and λ - X-ray wavelength.

1.3.2. Scanning Electron Microscopy (SEM)

The morphology of the powders and films was determined by scanning electron microscopy (SEM) using a Leica-Zeiss JEOL 7001F coupled with a spectrometer for energy-dispersive X-ray spectroscopy

(EDX) employed to study the morphology and elemental composition of the CIGS powders and films. The layer thickness was valued from cross-section micrographs.

1.3.3. Transmission and Reflection Spectra

In order to study the optical properties, the transmission and reflection spectra of CIGS thin films in the spectral range of 1000-2500 nm were examined using a UV-VIS-NIR Jasco 670 spectrophotometer.

2. Results and Discussion

The precursor powder prepared using the aqueous co-precipitation method was analyzed by SEM/EDX (Fig. 1). It can be observed that uniformly distributed small spherical particles with an average size > 30 nm were obtained. The crystal aggregates are inferior to 100 nm and suitable for further thin film deposition after a previous dispersion procedure to desegregate the agglomerates by ultrasonic bathing. The chemical composition analyzed by EDX corresponds to the initial stoichiometry (Cu/In/Ga = 1:0.78:0.33).

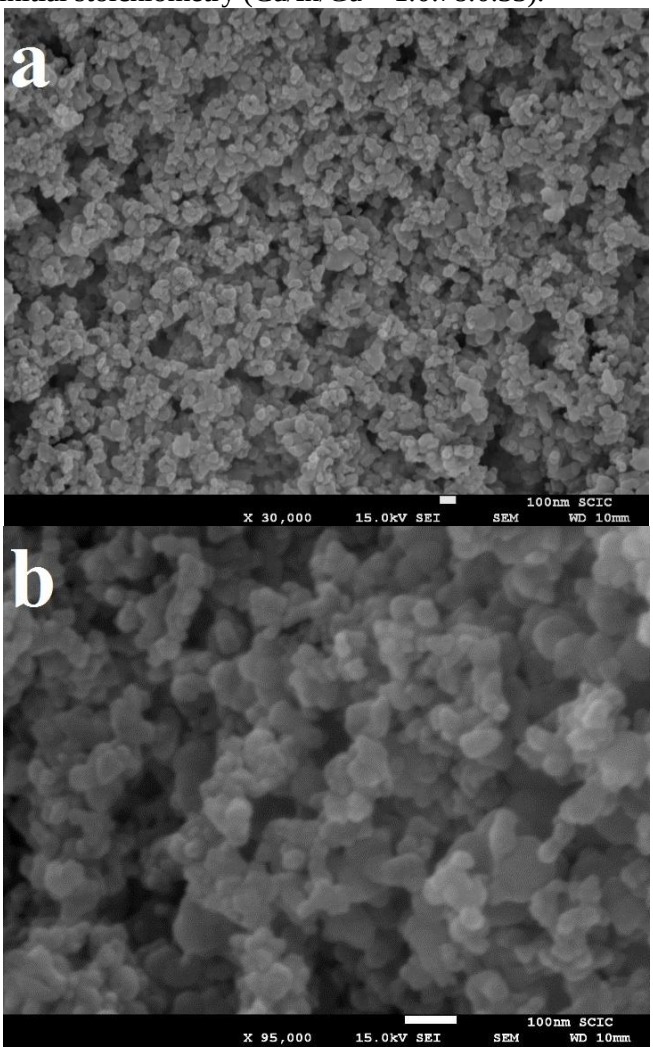

Fig. 1 SEM images of the prepared CIGS precursor powder: a) at 30000x; b) closer view 95000x (Developed by the authors)

The X-ray diffraction spectra of CIGS films treated at 525°C are exposed in Fig. 2. The diffraction peaks labeled with hkl could be assigned to $Cu(In_{0.7}Ga_{0.3})Se_2$ (CIGS) crystalline phase (JCPDS 35-1102). It can be highlighted that V1 exhibits a unique CIGS crystalline phase, while V2 contains some secondary phases labeled as (*) on the diffractogram. These additional peaks in sample V2 (the sample has three layers) could be associated to the formation of $Cu_{1.8}Se$ (JCPDS 96-900-8067) during the thermal selenization.

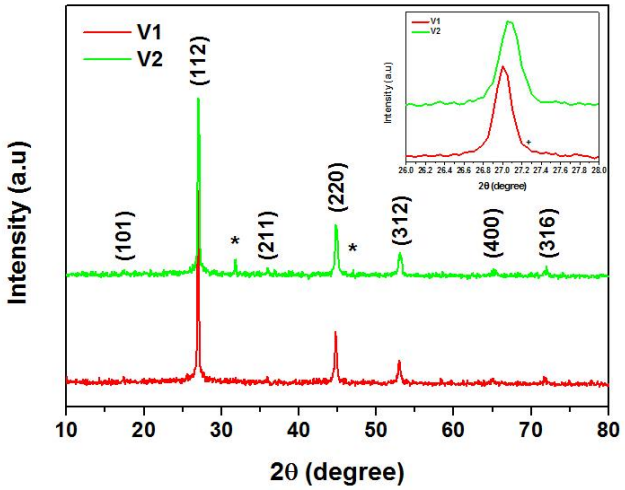

Fig. 2 XRD patterns of the CIGS layer after thermal treatment (Developed by the authors)

Fig. 3 and 4 show the SEM images (a - cross section, b - top-view) of the films. It displays that the CIGS layers are compact and adherent with uniform thickness close to 4.1 µm for sample V1 and 6.3 µm for sample V2 in accordance with the number of deposition steps.

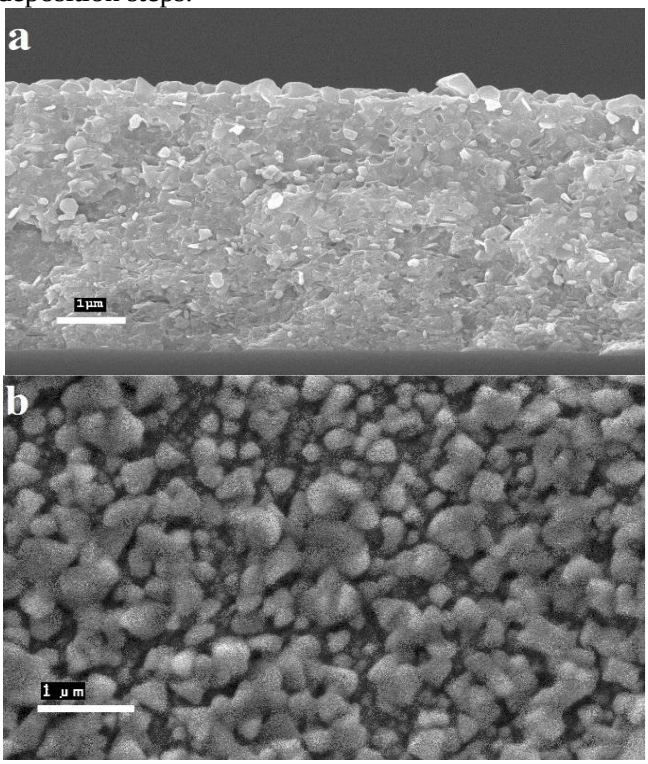

Fig. 3 SEM micrographs of sample V1: (a) cross section; (b) top-view (Developed by the authors)

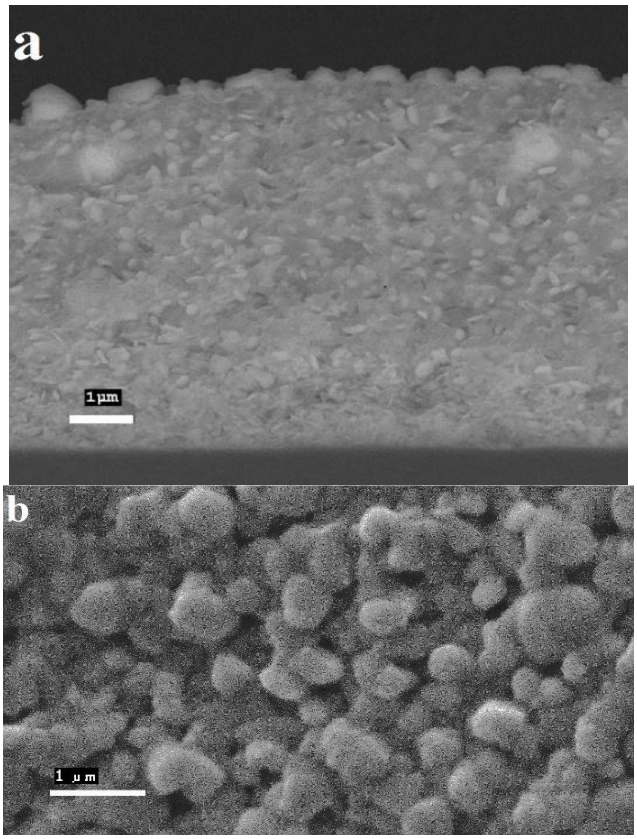

Fig. 4 SEM micrographs of sample V2: (a) cross section; (b) top-view (Developed by the authors)

The size of the particles is in the range of 200-250 nm in the volume and on the surface for the sample V1 is in the range of 200-680 nm and for the sample V2 - 330-930 nm. Their type is agglomerates composed of little crystal nanoparticles. In Table 1, the crystal nano-particle´s sizes are determined from the XRD spectra for the reflections hkl (112, 220, and 312). It can be noticed that the crystallites keep the initial size of around 30-40 nm of the precursor powder. The thermal treatment and the triethanolamine applied as surfactant inhibit the CIGS crystal growth. It is known that the amines act as reduction and gelatin agents [30, 31]. Reducers help to transform the precipitated selenite powder to selenides, while the gelatin effect helps to stabilize the paste for further layer deposition. However, further thermal treatment is applied to increase the sample crystallinity.

Table 1 Crystal sizes of samples V1 and V2 obtained from X-ray diffraction (Developed by the authors)

Sample	Pos./°2th	FWHM/°2th	Crystal size/nm
V1	27.00	0.2460	34.71
	44.75	0.2952	30.42
	52.95	0.3444	26.94
	65.30	0.3936	25.05
V2	27.05	0.1968	43.38
	35.95	0.2952	29.57
	44.80	0.2460	36.49
	53.10	0.1968	42.18

For the study of the optical properties of CIGS thin films, the transmission and reflection spectra were registered in the spectral range λ = 1000-2500 nm. The transmittance (Fig. 5a), T, of the thin film with thickness of 4.1 µm (sample V1) reaches 7.46% and this of the thin film with thickness of 6.3 µm (sample V2) - up to 4.56%. These results show that in this spectral range, the CIGS thin films absorb the incident light, and the absorption decreases as the wavelength increases and the films with greater thickness transmit less.

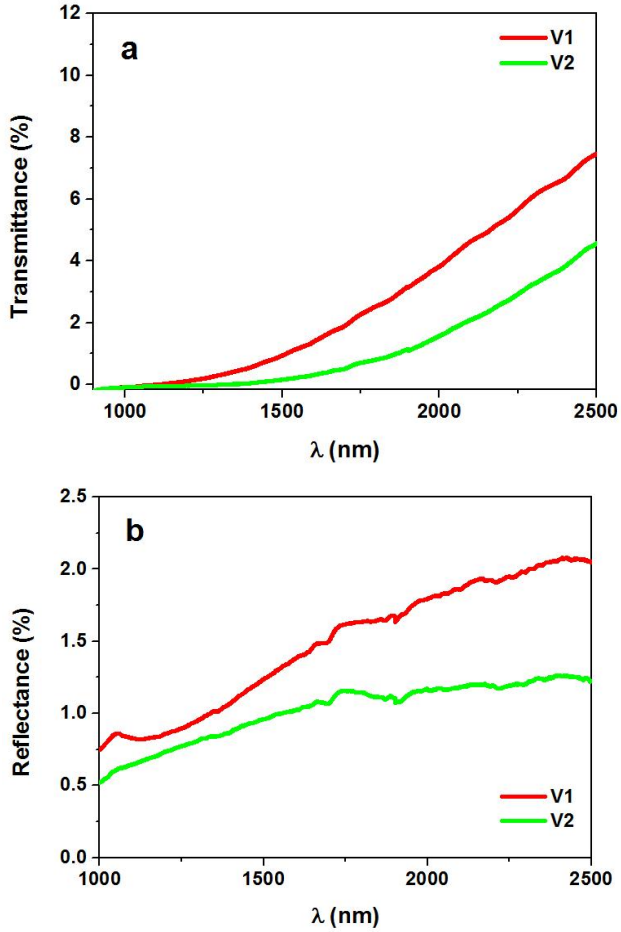

Fig. 5 CIGS thin films: (a) transmission and (b) reflection spectra (Developed by the authors)

In the same spectral range, the coefficient of reflection (Fig. 5b), R, of the sample V1 reaches 2.05% and these for the sample V2 - up to 1.23%. The results show that in this area the CIGS thin films slightly reflect the incident light. As the wavelength increases, the reflection coefficients increase and the films with greater thickness reflect less. The obtained results make the studied CIGS thin films suitable for use as absorbers in solar cells.

For a thin film without interference, with thickness *d*, refractive index *n*, extinction coefficient *k*, and absorption coefficient α in the case of normal-incidence light, the coefficients of transmission and reflection are calculated by the following formulas [32]:

$$T = \frac{(1-R_0)^2 x}{1-R_0^2 x^2}\left(1+\frac{k^2}{n^2}\right) \quad (2)$$

$$R = R_0\left(1+\frac{(1+R_0)^2\left(1+\frac{k^2}{n^2}\right)x^2}{1-R_0^2 x^2}\right) \quad (3)$$

$$R_0 = \frac{(n-1)^2+k^2}{(n+1)^2+k^2} \quad (4)$$

$$x = exp(-\alpha d) \quad (5)$$

Since in this study $n>>k$ according to [33], the above equations become

$$R_0 = \frac{(n-1)^2}{(n+1)^2} \quad (6)$$

$$T = \frac{(1-R_0)^2 x}{1-R_0^2 x^2} \quad (7)$$

$$R = R_0\frac{1+(1-2R_0)x^2}{1-R_0^2 x^2} \quad (8)$$

From these formulae for the refractive index, we derived

$$n = \frac{1+\sqrt{R_0}}{1-\sqrt{R_0}} \quad (9)$$

$$R_0 = \frac{1+2R-R^2+T^2-\sqrt{\left(1-2R+R^2-T^2\right)^2+4T^2}}{2(2-R)} \quad (10)$$

To obtain the refractive index values of the studied CIGS thin films, the values of the transmission and reflection coefficients of the received spectra were used. The spectral dependencies of refractive index of CIGS thin films are presented in Fig. 6. For both films, the refractive index increases with increasing wavelength (abnormal dispersion) as the thin layers in this part of the spectrum absorb the incident radiation.

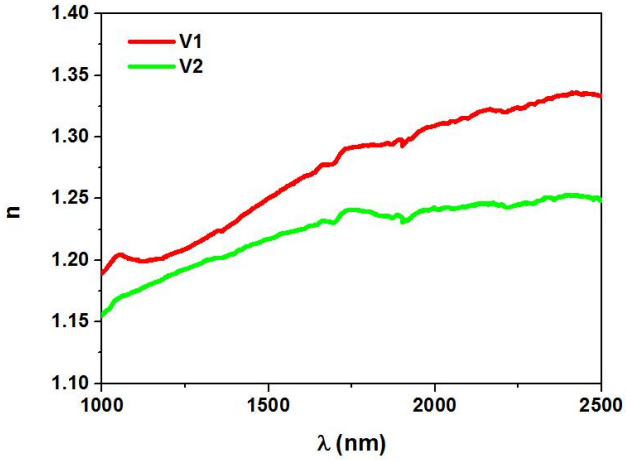

Fig. 6 Spectral dependencies of refractive index of CIGS thin films (Developed by the authors)

The refractive index values were calculated by Formula (9). For V1 CIGS thin films, they range from 1.189 to 1.336, and those of V2 CIGS thin films range from 1.155 to 1.253. It can be seen that the greater the film thickness, the smaller the values of the refractive index.

Based on [32, 33] the absorption coefficient of the studied CIGS thin films is estimated using the formula:

$$\alpha = -\frac{1}{d}ln\left(\frac{-1+2R-R^2+T^2+\sqrt{\left(1-2R+R^2-T^2\right)^2+4T^2}}{2T}\right) \quad (11)$$

The values of absorption coefficient were calculated with the values of coefficients of transmission and reflection of the obtained transmission and reflection spectra and the thickness values of the thin films. CIGS absorption coefficient values are in the range of 10^5-10^6 cm^{-1}. The smaller the thickness, the greater the absorption coefficient.

The spectral dependencies of absorption coefficient of CIGS thin films are presented in Fig. 7. Upon increasing the energy to 0.7 eV for V1 thin films and to 0.8 eV for V2 thin films, the absorption coefficient changes linearly, increasing with increasing energy. After these values, the change becomes exponential. From the spectra, it can be seen that the end of optical absorption for thicker films occurs at lower energies.

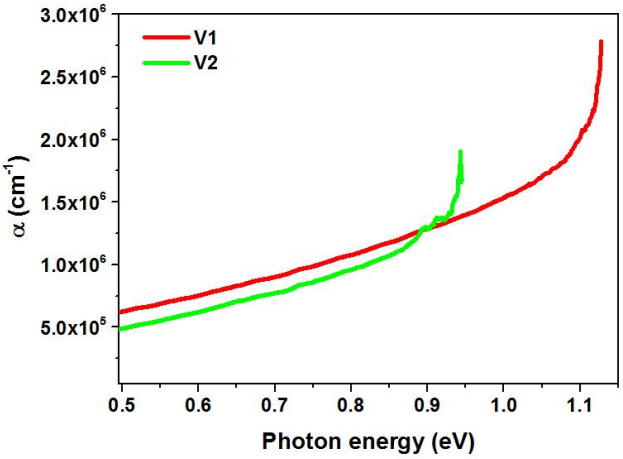

Fig. 7 Spectral dependencies of the absorption coefficient of CIGS thin films (Developed by the authors)

The absorption of light from the substance is characterized by the absorption coefficient. The expression of the coefficient of absorption α according to [34] has the following form:

$$\alpha(\nu) = B(h\nu - E_{opt})^r/h\nu \quad (12)$$

where ν is the light frequency, B - a constant, h - Planck's constant, E_{opt} - the optical band gap, and r - a step indicator that characterizes the mechanism of electron transition from the valence zone to the conductive zone.

To see what electron transitions occur in the CIGS thin films, we must find the degree of r by logarizing Expression (12):

$$ln(\alpha E) = r\, ln(BE - BE_{opt}) \quad (13)$$

A straight line equation is obtained in which the r rate is an angular factor (Fig. 8).

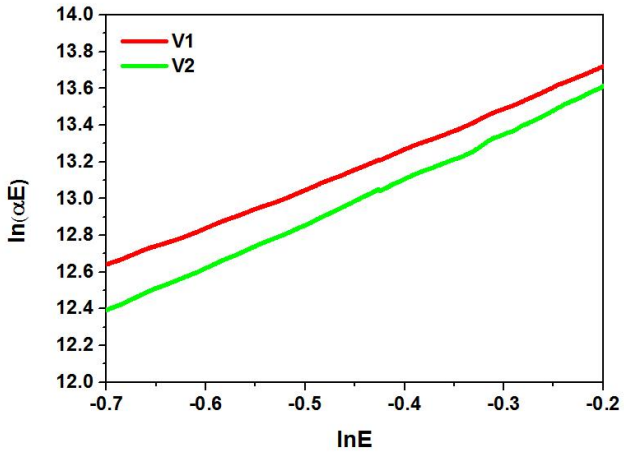

Fig. 8 Determining the types of electron transitions in CIGS thin films (Developed by the authors)

From Fig. 8, it was determined that r ≈ 2, i.e., the electron transitions from valence to conductive zone are indirect for all CIGS thin layers.

The end of optical absorption corresponds to the optical band gap. The values of the optical band gap E_{opt} for the CIGS thin films were calculated by extrapolating the slope of the $(\alpha E)^{1/2}$ curve vs. E at $(\alpha E)^{1/2} = 0$ according to Tauc's relation for the allowed indirect transition [29] (Fig. 9).

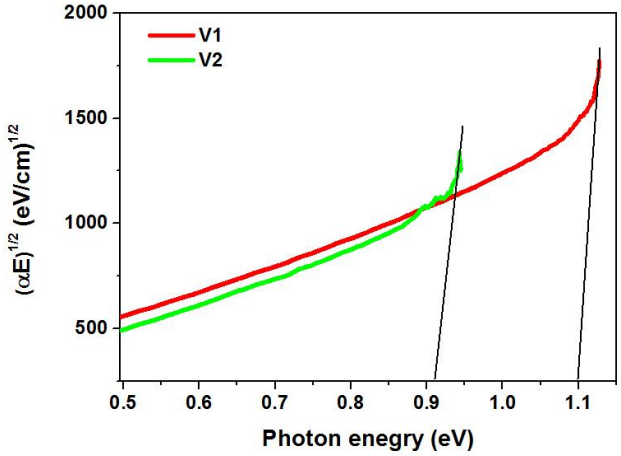

Fig. 9 Dependence of $(\alpha E)^{1/2}$ on photon energy E for the two different CIGS films from which the optical band gap Eopt is estimated (Tauc's extrapolation) (Developed by the authors)

Using Tauc's procedure for V1 CIGS thin layer, the optical band gap was estimated to be 1.10 eV and for V2 CIGS thin film - E_{opt} = 0.91 eV. The CIGS absorber band gap can be adjusted by tuning the composition ratio defined as [Ga]/([Ga] + [In]). The zoomed area in Fig. 2 displays a comparison of reflection (112) for the samples V1 and V2. It can be observed that for the sample V1 appears a small shoulder next to the principal peak. The presence of this shoulder at higher angles is related to gallium partial insertion (presence of gallium-rich phase). In the thicker layer (V2), the shoulder decreases, and the peak (112) is displaced toward higher angles. This is a confirmation of gallium incorporation into the crystal lattice [24]. Thus, the absorption band gap changes as a function of Ga incorporation into the crystal lattice (e.g. $Eg_{CuInSe2}$ is 1 eV, while $Eg_{CuGaSe2}$ is 1.7 eV). In summary, the sample V2 has Ga losses that also explain the XRD result (Fig. 2). The thicker layers have a smaller optical band gap, i.e., they will more easily and quickly transform the solar energy.

3. Conclusion

This study contributes to the field of optical properties of CIGS thin films deposed using a simple solution-based approach called the doctor blade technique. Using the doctor blade technique, homogeneous CIGS thin layers were obtained without three-dimensional defects such as pores, as confirmed by scanning electron spectroscopy. The transmission and reflection spectra of all CIGS thin films in the spectral range of 1000-2500 nm were studied. The value of the transmission coefficient *T* reaches 7.46%, and that of the reflection coefficient - up to 2.05%, which makes them suitable for use as absorbers in solar cells. The refractive index of the CIGS thin films was determined. Its value ranges from 1.155 to 1.336. The greater the film thickness, the smaller the value of the refractive index. For all thin layers, the refractive index increases with increasing wavelength (abnormal dispersion). The absorption coefficients were calculated. CIGS absorption coefficient values range from 10^5 to 10^6 cm^{-1}. The smaller the thickness, the greater the absorption coefficient. The end of optical absorption for the thicker films occurs at lower energies. Using Tauc's procedure for a CIGS thin layer with a thickness of 4.1 μm, the optical band gap was estimated to be 1.10 eV and for the CIGS thin films with a thickness of 6.3 μm - E_{opt} = 0,91 eV. The thicker layers have a smaller optical band gap, i.e., they will more easily and quickly transform the solar energy. To improve the optical parameters, one can work in two directions: increasing the thickness of thin films and reducing the amount of added gallium.

Acknowledgement

This study was funded by the European Union-NextGenerationEU through the National Recovery and Resilience Plan of the Republic of Bulgaria, Project № BG-RRP-2.004-0002 "BiOrgaMCT".

References

[1] FERNÁNDEZ A. M. & BHATTACHARYA R. Electrodeposition of $CuIn_{1-x}Ga_xSe_2$ precursor films: optimization of film composition and morphology. *Thin Solid Films*, 2005, 474(1-2): 10-13. https://doi.org/10.1016/j.tsf.2004.02.104

[2] BHATTACHARYA R. N., BATCHELOR W., GRANATA J. E., HASOON F., WIESNER H., RAMANATHAN K., KEANE J., and NOUFI R. N. $CuIn_{1-x}Ga_xSe_2$-based photovoltaic cells from electrodeposited and chemical bath deposited precursors. *Solar Energy Materials and Solar Cells*, 1998, 55(1-2): 83-

94. https://doi.org/10.1016/S0927-0248(98)00049-X
[3] BOUABID K., IHLAL A., MANAR A., OUTZOURHIT A., and AMEZIANE E. L. Effect of deposition and annealing parameters on the properties of $CuIn_{1-x}Ga_xSe_2$ thin films. *Thin Solid Films,* 2005, 488(1-2): 62-67. https://doi.org/10.1016/j.tsf.2005.04.111
[4] WADA T., HASHIMOTO Y., NISHIWAKI S., SATOH T., HAYASHI S., NEGAMI T., and MIYAKE H. High-efficiency CIGS solar cells with modified CIGS surface. *Solar Energy Materials and Solar Cells,* 2001, 67(1-4): 305-310. https://doi.org/10.1016/S0927-0248(00)00296-8
[5] CONTRERAS M. A., EGGAS B., RAMANATHAN K., HILTNER J., SWARTZLANDER A., HASOON F., and NOUFI R. Progress toward 20% efficiency in $Cu(In,Ga)Se_2$ polycrystalline thin-film solar cells. *Progress in Photovoltaics,* 1999, 7: 311-316. https://doi.org/10.1002/(SICI)1099-159X(199907/08)7:4<311::AID-PIP274>3.0.CO;2-G
[6] RAMANATHAN K., TEETER G., KEANE J. C., and NOUFI R. Properties of high-efficiency $CuInGaSe_2$ thin film solar cells. *Thin Solid Films,* 2005, 480-481: 499-502. https://doi.org/10.1016/j.tsf.2004.11.050
[7] KATO T., WU J.-L., HIRAI Y., SUGIMOTO H., and BERMUDEZ V. Record efficiency for thin-film polycrystalline solar cells up to 22.9% achieved by Cs-treated $Cu(In,Ga)(Se,S)_2$. *IEEE Journal of Photovoltaics,* 2019, 9(1): 325-330. https://doi.org/10.1109/JPHOTOV.2018.2882206
[8] MARTÍ R., OLIVEIRA L., STOYANOVA LYUBENOVA T., TODOROV T., CHASSAING E., LINCOT D., and CARDAV J. B. Preparation of $Cu(In,Ga)Se_2$ photovoltaic absorbers by an aqueous metal selenite co-precipitation route. *Journal of Alloys and Compounds,* 2015, 650: 907-911. https://doi.org/10.1016/j.jallcom.2015.08.014
[9] NADENAU V., BRAUNGER D., HARISKOS D., KAISER M., KÖBLE Ch., OBERACKER A., RUCKH M., RÜHLE U., SCHÄFFLER R., SCHMID D., WALTER T., ZWEIGART S., and SCHOCK H. W. Solar cells based on $CuInSe_2$ and related compounds: material and device properties and processing. *Progress in Photovoltaics,* 1995, 3: 363-382. https://doi.org/10.1002/pip.4670030602
[10] TUTTLE J. R., CONTRERAS M. A., GABOR A. M., RAMANATHAN K. R., TENNAT A. L., ALBIN D. S., KEANE J., and NOUFI R. Perspective on high-efficiency $Cu(In,Ga)Se_2$-based thin-film solar cells fabricated by simple, scalable processes. *Progress in Photovoltaics,* 1995, 3: 383-391. https://doi.org/10.1002/pip.4670030603
[11] CONTRERAS M., TUTTLE J., GABOR A., TENNAT A., RAMANATHAN K., ASHER S., FRANZ A., KEANE J., WANG L., and NOUFI R. High efficiency graded bandgap thin-film polycrystalline $Cu(In,Ga)Se_2$-based solar cells. *Solar Energy Materials and Solar Cells,* 1996, 41-42: 231-246. https://doi.org/10.1016/0927-0248(95)00145-X
[12] LIU J., ZHUANG D., LUAN H., CAO M., XIE M., and LI X. Preparation of $Cu(In,Ga)Se_2$ thin film by sputtering from $Cu(In,Ga)Se_2$ quaternary target. *Progress in Natural Science: Materials International,* 2013, 23(2): 133-138. https://doi.org/10.1016/j.pnsc.2013.02.006
[13] NIE M. & ELLMER K. Growth and morphology of thin $Cu(In,Ga)S_2$ films during reactive magnetron co-sputtering. *Thin Solid Films,* 2013, 536: 172-178. https://doi.org/10.1016/j.tsf.2013.03.118
[14] LEE D.-Y., PARK S., and KIM J. H. Structural analysis of CIGS film prepared by chemical spray deposition. *Current Applied Physics,* 2011, 11(1): S88-S92. https://doi.org/10.1016/j.cap.2010.11.089
[15] MAHENDRAN C. & SURIYANARAYANAN N. Effect of Bi incorporation and temperature on the properties of sprayed $CuInS_2$ thin films. *Physica B: Condensed Matter,* 2013, 408: 62-67. https://doi.org/10.1016/j.physb.2012.08.045
[16] KAMPMANN A., SITTNGER V., RECHID J., and REINEKE-KOCH R. Large area electrodeposition of $Cu(In,Ga)Se_2$. *Thin Solid Films,* 2000, 361-362: 309-313. https://doi.org/10.1016/S0040-6090(99)00863-9
[17] KAPUR V. K., BANSAL A., LE P., and ASENSIO O. I. Non-vacuum processing of $CuIn_{1-x}Ga_xSe_2$ solar cells on rigid and flexible substrates using nanoparticle precursor inks. *Thin Solid Films,* 2003, 431-432: 53-57. https://doi.org/10.1016/S0040-6090(03)00253-0
[18] FARAJ M. G., IBRAHIM K., and SALHIN A. Effects of Ga concentration on structural and electrical properties of screen printed-CIGS absorber layers on polyethylene terephthalate. *Materials Science in Semiconductor Processing,* 2012, 15(2): 206-213. https://doi.org/10.1016/j.mssp.2012.03.002
[19] CHIHI A., BOUJMIL M. F., and BESSAIS B. Optical and electrical characterization of CIGS thin films grown by electrodeposition route. *Optik,* 2016, 127(8): 4118-4122. https://doi.org/10.1016/j.ijleo.2016.01.115
[20] LUO P., ZHU C., and JIANG G. Preparation of $CuInSe_2$ thin films by pulsed laser deposition the Cu–In alloy precursor and vacuum selenization. *Solid State Communications,* 2008, 146(1-2): 57-60. https://doi.org/10.1016/j.ssc.2008.01.020
[21] GUILLÉN C. & HERRERO J. Semiconductor $CuInSe_2$ formation by close-spaced selenization processes in vacuum. *Vacuum,* 2002, 67(3-4): 659-664. https://doi.org/10.1016/S0042-207X(02)00258-0
[22] CALIXTO M. E., DOBSON K. D., MCCANDLESS B. E., and BIRKMIRE R. W. Controlling growth chemistry and morphology of single-bath electrodeposited $Cu(In,Ga)Se_2$ thin films for photovoltaic application. *Journal of the Electrochemical Society,* 2006, 153: G521-G528. https://doi.org/10.1149/1.2186764
[23] CHEN C., QI X., CHANG W., TSAI M., CHEN I., LIN C., WU P., and CHANG K. The effects of pulse repetition rate on the structural, optical, and electrical properties of CIGS films grown by pulsed laser deposition. *Applied Surface Science,* 2015, 351: 772-778. https://doi.org/10.1016/j.apsusc.2015.06.002
[24] CHANDRAMOHAN M., VELUMANI S., and VENKATACHALAM T. Experimental and theoretical investigations of structural and optical properties of CIGS thin films. *Materials Science and Engineering: B,* 2010, 174(1-3): 205-208. https://doi.org/10.1016/j.mseb.2010.03.041
[25] OLIVEIRA L., LYUBENOVA T., MARTÍ R., FRAGA D., REY A., KOZHUKHAROV V., and CARDA J. In-situ sol-gel synthesis and thin film deposition of $Cu(In,Ga)(S,Se)_2$ solar cells. *Journal of Chemical Technology and Metallurgy,* 2013, 48(6): 559-566. https://journal.uctm.edu/node/j2013-6/3-Oliveira_559-566.pdf
[26] TODOROV T. & MITZI D. B. Direct liquid coating of chalcopyrite light-absorbing layers for photovoltaic devices. *European Journal Inorganic Chemistry,* 2010, 2010(1): 17-

28. https://doi.org/10.1002/ejic.200900837
[27] BERNI A., MENNING M., and SCHMIDT H. Doctor Blade. In: AEGERTER M. A. & MENING M. (eds.) *Sol-Gel Technologies for Glass Producers and Users.* Springer, Boston, Massachusetts, 2004: 89-92. https://doi.org/10.1007/978-0-387-88953-5_10
[28] REPINS I., CONTRERAS M. A., EGAAS B., DEHART C., SCHARF J., PERKINS C. L., TO B., and NOUFI R. 19·9%-efficient ZnO/CdS/CuInGaSe^2 solar cell with 81·2% fill factor. *Progress in Photovoltaics*, 2008, 16(3): 235-239. https://doi.org/10.1002/pip.822
[29] TAUC J. *Optical Properties of Solids.* North-Holland, Amsterdam, 1972.
[30] BASOL B. M., KAPUR V. K., HALANI A. T., LEIDHOLM C. R., and ROE R. A. *Method of making compound semiconductor films and making related electronic devices.* 1999. https://patents.google.com/patent/US5985691A/en
[31] CURTIN T., O'REGAN F., DECONINCK C., KNÜTTLE N., and HODNETT B. K. The catalytic oxidation of ammonia: influence of water and sulfur on selectivity to nitrogen over promoted copper oxide/alumina catalysts. *Catalysis Today*, 2000, 55(1-2): 189-195. https://doi.org/10.1016/S0920-5861(99)00238-2
[32] DRESSEL M. & GRÜNER G. *Electrodynamics of Solids: Optical Properties of Electrons in Matter.* Cambridge University Press, Cambridge, 2002.
[33] LILOV E., LILOVA V., and NEDEV S. Optical band gap dependence on the oxalic acid concentration of antimony anodic oxide films. *Bulgarian Chemical Communications*, 2016, 48(Special Issue G): 17-20. http://bcc.bas.bg/BCC_Volumes/Volume_48_Special_G_2016/BCC-48-G-2016-17-20-s3-PA3.pdf
[34] MOTT N. F. and DAVIS E. A. *Electronic processes in non-crystalline materials.* Clarendon Press, Oxford, 1979.

参考文:

[1] FERNÁNDEZ A. M. & BHATTACHARYA R. 铜铟 1−硒化镓前驱体薄膜的电沉积：薄膜成分和形态的优化。固体薄膜，2005，474(1-2)：10-13。https://doi.org/10.1016/j.tsf.2004.02.104
[2] BHATTACHARYA R. N.、BATCHELOR W.、GRANATA J. E.、HASOON F.、WIESNER H.、RAMANATHAN K.、KEANE J. 和 NOUFI R.N. 来自电沉积和化学浴沉积前体的基于铜铟 1−硒化镓 的光伏电池。太阳能材料与太阳能电池，1998，55(1-2)：83-94。https://doi.org/10.1016/S0927-0248(98)00049-X
[3] BOUABID K.、IHLAL A.、MANAR A.、OUTZOURHIT A. 和 AMEZIANE E. L. 沉积和退火参数对铜铟 1−硒化镓薄膜性能的影响。固体薄膜，2005，488(1-2)：62-67。https://doi.org/10.1016/j.tsf.2005.04.111
[4] WADA T.、HASHIMOTO Y.、NISHIWAKI S.、SATOH T.、HAYASHI S.、NEGAMI T. 和 MIYAKE H. 具有改性 CIGS 表面的高效 CIGS 太阳能电池。太阳能材料与太阳能电池，2001，67(1-4)：305-310。https://doi.org/10.1016/S0927-0248(00)00296-8
[5] CONTRERAS M. A.、EGGAS B.、RAMANATHAN K.、HILTNER J.、SWARTZLANDER A.、HASOON F. 和 NOUFI R。铜(铟、镓) 硒多晶薄膜太阳能电池效率达到 20% 的进展。光伏进展，1999，7：311-316。https://doi.org/10.1002/(SICI)1099-159X(199907/08)7:4<311::AID-PIP274>3.0.CO;2-G
[6] RAMANATHAN K.、TEETER G.、KEANE J.C. 和 NOUFI R. 高效铜铟镓硒薄膜太阳能电池的特性。固体薄膜，2005，480-481：499-502。https://doi.org/10.1016/j.tsf.2004.11.050
[7] KATO T.、WU J.-L.、HIRAI Y.、SUGIMOTO H. 和 BERMUDEZ V. 通过 Cs 处理的铜(铟、镓)实现薄膜多晶太阳能电池效率高达 22.9%的记录(硒,硫)2。IEEE 光伏杂志，2019，9(1)：325-330。https://doi.org/10.1109/JPHOTOV.2018.2882206
[8] MARTÍ R.、OLIVEIRA L.、STOYANOVA LYUBENOVA T.、TODOROV T.、CHASSAING E.、LINCOT D. 和 CARDAV J. B. 通过水性金属亚硒酸盐共沉淀法制备铜(铟、镓) 硒光伏吸收体 路线。合金与化合物杂志，2015，650：907-911。https://doi.org/10.1016/j.jallcom.2015.08.014
[9] NADENAU V.、BRAUNGER D.、HARISKOS D.、KAISER M.、KÖBLE Ch.、OBERACKER A.、RUCKH M.、RÜHLE U.、SCHäFFLER R.、SCHMID D.、WALTER T.、ZWEIGART S.，以及 SCHOCK H. W. 基于硒化铜和相关化合物的太阳能电池：材料和器件特性及加工。光伏发电进展，1995，3：363-382。https://doi.org/10.1002/pip.4670030602
[10] TUTTLE J. R., CONTRERAS M. A., GABOR A. M., RAMANATHAN K. R., TENNAT A. L., ALBIN D. S., KEANE J., 和 NOUFI R. 对高效铜(铟、镓) 硒基薄膜太阳能电池的展望 简单、可扩展的流程。光伏发电进展，1995，3：383-391。https://doi.org/10.1002/pip.4670030603
[11] CONTRERAS M., TUTTLE J., GABOR A., TENNAT A., RAMANATHAN K., ASHER S., FRANZ A., KEANE J., WANG L., 和 NOUFI R. 高效分级带隙薄膜多晶铜(铟、镓)硒基太阳能电池。太阳能材料和太阳能电池，1996，41-42：231-246。https://doi.org/10.1016/0927-0248(95)00145-X
[12] 刘健，庄大，栾华，曹明，谢明，李 X. 铜(铟、镓) 硒四元靶材溅射制备铜(铟、镓) 硒薄膜。自然科学进展：材料国际，2013，23(2)：133-138. https://doi.org/10.1016/j.pnsc.2013.02.006
[13] NIE M. & ELLMER K. 反应磁控管共溅射过程中铜(铟、镓)S2 薄膜的生长和形貌。固体薄膜，2013 年，536：172-178。https://doi.org/10.1016/j.tsf.2013.03.118
[14] LEE D.-Y.，PARK S.，和 KIM J. H. 化学喷雾沉积制备的 CIGS 薄膜的结构分析。当前应用物理，2011，11（1）：S88-S92。https://doi.org/10.1016/j.cap.2010.11.089
[15] MAHENDRAN C. & SURIYANARAYANAN N. 双掺入和温度对喷涂硫化铜薄膜性能的影响。物理学乙：凝聚态物质，2013，408：62-67。https://doi.org/10.1016/j.physb.2012.08.045
[16] KAMPMANN A.、SITTNGER V.、RECHID J. 和 REINEKE-KOCH R. 铜(铟、镓) 硒的大面积电沉积。固体薄膜，2000 年，361-362：309-313。https://doi.org/10.1016/S0040-6090(99)00863-9
[17] KAPUR V. K.、BANSAL A.、LE P. 和 ASENSIO O. I. 使用纳米颗粒前驱体墨水对刚性和柔性基板上的铜铟 1−硒化镓太阳能电池进行非真空加工。固体薄膜，2003

年， 431-432 ： 53-57 。 https://doi.org/10.1016/S0040-6090(03)00253-0
[18] FARAJ M. G.、IBRAHIM K. 和 SALHIN A. 嘎浓度对聚对苯二甲酸乙二醇酯上丝网印刷 CIGS 吸收层的结构和电性能的影响。半导体加工材料科学，2012，15(2)：206-213. https://doi.org/10.1016/j.mssp.2012.03.002
[19] CHIHI A.、BOUJMIL M. F. 和 BESSAIS B. 通过电沉积途径生长的 CIGS 薄膜的光学和电学特性。光学，2016，127(8)：4118-4122 。https://doi.org/10.1016/j.ijleo.2016.01.115
[20] LUO P.，ZHU C.，和 JIANG G. 通过脉冲激光沉积铜铟合金前驱体和真空硒化制备硒化铜薄膜。固态通信，2008，146(1-2)：57-60 。https://doi.org/10.1016/j.ssc.2008.01.020
[21] GUILLÉN C. & HERRERO J. 通过真空中近距离硒化过程形成半导体硒化铜。真空，2002，67(3-4)：659-664 。https://doi.org/10.1016/S0042-207X(02)00258-0
[22] CALIXTO M. E.、DOBSON K. D.、MCCANDLESS B. E. 和 BIRKMIRE R. W. 控制光伏应用单浴电沉积铜(铟、镓) 硒薄膜的生长化学和形态。电化学会杂志，2006，153：G521-G528 。https://doi.org/10.1149/1.2186764
[23] 陈成，齐 X.，张伟，蔡明，陈一，林成，吴鹏，张 K.脉冲重复率对结构、光学和电学性质的影响 通过脉冲激光沉积生长的 CIGS 薄膜。应用表面科学，2015，351：772-778。https://doi.org/10.1016/j.apsusc.2015.06.002
[24] CHANDRAMOHAN M. 、VELUMANI S. 和 VENKATACHALAM T. CIGS 薄膜结构和光学特性的实验和理论研究。材料科学与工程: 乙, 2010, 174(1-3): 205-208. https://doi.org/10.1016/j.mseb.2010.03.041
[25] OLIVEIRA L., LYUBENOVA T., MARTÍ R., FRAGA D., REY A., KOZHUKHAROV V., 和 CARDA J. 铜(铟、镓) (的原位溶胶-凝胶合成和薄膜沉积)(硫、硒)2 太阳能电池。化工冶金学报，2013，48(6)：559-566. https://journal.uctm.edu/node/j2013-6/3-Oliveira_559-566.pdf
[26] TODOROV T. & MITZI D. B. 用于光伏器件的黄铜矿光吸收层的直接液体涂层。欧洲无机化学杂志，2010，2010（1）：17-28 。https://doi.org/10.1002/ejic.200900837
[27] BERNI A.、MENNING M. 和 SCHMIDT H. 刀刃博士。见：AEGERTER M. A. 和 MENING M.（编辑）面向玻璃生产商和用户的溶胶-凝胶技术。施普林格，马萨诸塞州波士顿，2004 年：89-92 。https://doi.org/10.1007/978-0-387-88953-5_10
[28] REPINS I.、CONTRERAS M. A.、EGAAS B.、DEHART C.、SCHARF J.、PERKINS C. L.、TO B. 和 NOUFI R. 效率 19•9%的氧化锌/硫化镉/铜铟镓硒太阳能电池，效率为 81•2%填充因子。光伏进展，2008，16(3)：235-239。https://doi.org/10.1002/pip.822
[29] TAUC J. 固体的光学性质。北荷兰省，阿姆斯特丹，1972 年。
[30] BASOL B.M.、KAPUR V.K.、HALANI A.T.、LEIDHOLM C.R.和 ROE R.A. 制造化合物半导体薄膜和制造相关电子器件的方法。1999 。https://patents.google.com/patent/US5985691A/en
[31] CURTIN T.、O'REGAN F.、DECONINCK C.、KNÜTTLE N. 和 HODNETT B.K. 氨的催化氧化：水和硫对促进的氧化铜/氧化铝催化剂上氮选择性的影响。今日催化，2000，55(1-2)：189-195 。https://doi.org/10.1016/S0920-5861(99)00238-2
[32] DRESSEL M. & GRÜNER G. 固体电动力学：物质中电子的光学性质。剑桥大学出版社，剑桥，2002 年。
[33] LILOV E.、LILOVA V. 和 NEDEV S. 光学带隙对锑阳极氧化膜草酸浓度的依赖性。保加利亚化学通讯，2016，48（特刊 G）：17-20 。http://bcc.bas.bg/BCC_Volumes/Volume_48_Special_G_2016/BCC-48-G-2016-17-20-s3-PA3.pdf
[34] MOTT N. F. 和 DAVIS E. A. 非晶材料中的电子过程。克拉伦登出版社，牛津，1979 年。